CROATICA CHEMICA ACTA CCACAA **65** (2) 309–326 (1992)

ISSN 0011-1643
UDC 541.1
CCA–2061 *Original Scientific Paper*

Electrolyte and Polyelectrolyte Induced Aggregation of Colloids. Mechanism of Colloid Destabilization

E. Pefferkorn

Institut Charles Sadron 6, Rue Boussingault, 67083 Strasbourg, (Cédex), France

Received October 21, 1991

Spherical latex particles were used as a colloid model to investigate the aggregation process resulting from the action of electrolytes and polyelectrolytes. The colloid size distribution was directly determined using a particle counter technique. Bell shaped curves were expected for diffusion limited aggregation (DLA) when particle sticking succeeded each interparticle collision. The colloid size frequency was described by a continuously decreasing curve when reaction limited aggregation (RLA) was expected. The last mode implied that the collision efficiency for sticking might depend on the aggregate size. Starting with the cluster size distribution, we calculated the different moments of the size distribution.

When electrostatic forces modulated the interparticle interactions, in the presence of a excess of electrolyte or at a polymer concentration inducing fast aggregation, the reduced size distribution exhibited a typical maximum and the aggregation kinetic was described by a simple scaling law. As a result, a time invariant size polydispersity characterized the long time behavior. Apart from these ideal coagulation conditions, the flocculation proceeded at a slower rate and the dynamic scaling laws required two scaling exponents, w and z. The cluster size polydispersity factor increased with aggregation period as a result of variable collision efficiency.

When flexible polymer acted as an interparticle bridging agent, the amount of polymer adsorbed on a colloid surface also modulated the rate of aggregation but the aggregation mode itself was only determined by the polymer/colloid interaction. Fast aggregation was found to induce maximal cluster size polydispersity.

In all these situations, colloid aggregation modes were analyzed using the results of computer simulation of the cluster-cluster aggregation and the experimental results were presented *via* a scaling approach. Validity of scaling relations was verified for electrolyte and polyelectrolyte induced aggregation and the different processes corresponded to diffusion and reaction limited aggregation.

INTRODUCTION

Mechanisms of colloid aggregation have been studied theoretically and by computer simulation, starting from the binary collision model of von Smoluchowski, to predict the modes of clustering from consideration of the rate of aggregate growth.[1] Starting from the particle-cluster aggregation, the model of Witten and Sander,[2] later developed into cluster-cluster aggregation by Meakin,[3] and independently by Kolb, Botet and Jullien,[4] computer simulation established the static and hydrodynamic characteristics of clusters and the dynamic laws of aggregation.

Two kinetic processes were examined: DLA[5-13] and RLA[14-18] cluster-cluster aggregation and, in the context of this paper, we mainly refer to the results of simulation relative to the time dependent cluster size distribution. In order to obtain temporal evolution of the size of real aggregates in electrolyte and polyelectrolyte induced aggregation, we used a particle counter technique directly furnishing this information. Although characteristic aggregation experiments induced by electrolyte have been previously investigated,[19-27] our aim was to compare the modes of destabilizing action of electrolyte and polyelectrolyte.

The possible modes of action of polymeric flocculants are well known, but the acting process depends on the experimental conditions imposing both the colloid charge and the structure and charge of the adsorbed layer. Therefore, in most situations, it is difficult to attribute the destabilizing effect to a defined mechanism. One possible mode arises from the high selectivity coefficient of this multivalent macro-ion towards charged colloids; the polyelectrolyte replaces most of the small counter-ions of the diffuse layer and, thus, it is able to induce effects similar to those resulting from electrolytes. We conjecture that the optimum polymer dosage may be comparable to the situation of excess electrolyte and leads to a polymer/colloid complex of zero net charge. Evidence is provided by the finding that the dosage of optimal flocculation corresponds to zero mobility in microelectrophoresis measurements.[28,29]

Apart from these conditions, the mechanism of destabilization is not properly known. When a charged colloid is suspended in dilute or concentrated polyelectrolyte solutions, the surface charge may be inadequately screened and, thus, the repulsive effect of residual electrostatic charges – belonging to the colloid in the presence of a default of polyelectrolyte and to the adsorbed polyelectrolyte in the case of an excess of polymer – contributes to slowing down of the aggregation rate. Electrostatic forces contravene van der Waals attraction between colliding colloids. In the second mode of action, polymers are able to link together two or more colloidal particles. Interparticle bridging may be expected to occur when the surface possesses a low density of charge and the polyelectrolyte adopts an extended structure due to a high degree of ionization.[30,31]

Our first aim was to investigate if polyelectrolyte induced aggregation may be analyzed by the scaling approach like electrolyte induced aggregation and, secondly, we were interested in the determination of the dynamic scaling exponents characterizing the temporal variation of the different moments N_i (i = 0, 1 and 2) of the cluster size distribution for aggregation performed under different conditions. Therefore, we determined the aggregate concentration as a function of the number of constitutive elementary particles. This parameter was recorded as a function of the aggregation time and denoted $c_n(t)$. A knowledge of the aggregate size distribution permitted calculation of the average characteristics of the colloid:

- the average weight size $N_2(t)/N_1$
- the average number size $N_1/N_0(t)$
- the size polydispersity factor $N_2(t)N_1(t)/N_1^2$.

We note that this information is similar to that obtained in computer simulation and to interpret our experimental results we refer to dynamic scaling laws established in simulation studies of diffusion and reaction limited cluster-cluster aggregation processes in a three-dimensional space. Materials and techniques are described first and then the characteristics of the DLA and RLA processes are outlined.

MATERIALS AND METHODS

Electrolyte: Sodium chloride (Suprapur, Merck) was used as a low molecular weight destabilizing agent.

Polyelectrolyte: Poly(vinyl-2-pyridine) (PVP) constituted a model of water soluble flexible polymer and a fractionated sample of molecular weight $3.6 \cdot 10^5$ was selected. PVP protonation is a function of the pH of the solution and the polymer is fully protonated in strong acid solution. The limiting condition of PVP solubility is pH 4, where protonation is zero. At intermediate pH, the degree of protonation α was calculated on the basis of spectroscopic measurements at 253 nm, using the following relationship:

$$\varepsilon = \varepsilon_p (1 - \alpha) + \varepsilon_{p+} \cdot \alpha \tag{1}$$

ε_p being the molar extinction coefficient of the pyridine group (determined at pH 4), and ε_{p+} the molar extinction coefficient of the pyridinium group (determined at pH 0). At the pH value of 2.5 and 3.0, the degree of pyridine protonation is 0.730 and 0.475, respectively.[32]

Colloid: Monosized latex particles were kindly furnished by the Laboratoire des Materiaux Organiques of Lyon (France). They were polymerized under emulsifier-free conditions, using potassium persulfate as free radical initiator.[33] Two samples were used:

- latex (a) had SO_4^{2-}, COO^- and OH surface groups. The point zero charge (pzc) was found to be 3.0, so that at pH 3.5 the latex bore a net negative charge. However, in acidic medium, proton adsorption on hydroxyl groups may lead to an amphoteric surface bearing both positive and negative electrical charges.
- latex (b), obtained by hydrolysis of latex (a) at 90 °C for 7 days, bore only carboxylic acid surface groups. The pzc was found to be close to 2.4. The density of the lattices was 1.045 g/ml and the mean particle diameter was determined by quasielastic light scattering and electron microscopy and confirmed, by particle counting, to be 900 nm.

In order to characterize the net surface ionization of lattices (a) and (b) as a function of pH, the surface potential was determined by the method of Malvern (Zeta Sizer 3) and the values are reported in Figure 1.

Aggregation Procedure: All experiments were performed at a constant concentration of 0.16 g latex/l at 18 °C. Following the usual procedures, the latex suspension was added to the electrolyte and polyelectrolyte solutions and gentle tumbling was performed twice before perikinetic flocculation started. In order to eliminate particle sedimentation, which sets in slowly when the latex is suspended in pure water and which would disturb an experiment designed to study perikinetic flocculation, experiments were performed in a mixture of (D_2O/H_2O) (57g/47g) having the same density as the latex.

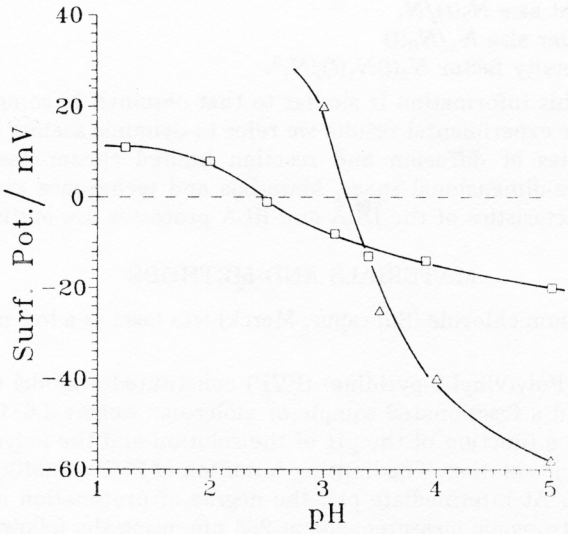

Figure 1. Surface potential Ψ of latex (a) (Δ) and latex (b) (□) as a function of pH.

Particle Counting: The Coulter Counter is able to measure the size of individual particles and clusters in very dilute suspension (for counting, the suspension is diluted up to one hundred times).[34] The principle of counting is that the particle moves in a suspending electrolyte (NaCl, 0.15 M) through a constricted electrical current path. An aperture is set in the wall of an insulated vessel and direct current is applied across a pair of electrodes, one situated inside the insulated vessel, the other outside in the suspension of identical electrolyte concentration. The passage of each species causes an increase in resistance across the electrodes. The corresponding voltage pulse is proportional to the volume of matter and is simplified for display on an oscilloscope and for feeding to a pulse height discriminator and a set of sixteen counters.

The aperture has a diameter of 50 μm and allows determination of the size of particles as small as 0.79 μm in the second channel (the first channel accumulates some background that has to be discarded). Fifteen channels are, thus, available for size analysis and the standardization is elaborated as depicted below:

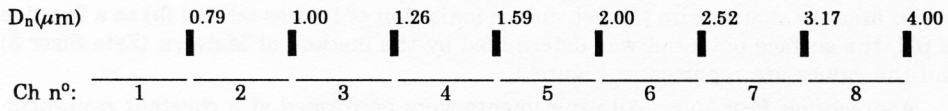

In the upper line, the threshold diameters of particles are indicated, which are »collected« in successive channels, numbered in the lower line. The apparatus was calibrated only to collect elementary particles in channel 2, aggregates of two, three and more particles appearing in the third and following channels. Thus, channel 2 gives information relating to the concentration of individual dispersed particles even in the presence of aggregates. In fact, due to the small original latex polydispersity and/or

the presence of a small number of doublets and triplets, analysis of a stable suspension shows the presence of some species in channel 3.

Precautions were taken in order to perform non-destructive size distribution analyses and sampling of small parts of the colloid suspension was done with a special syringe at a shear rate smaller than 10 s^{-1}. For electrolyte induced aggregation, samples of the aggregating suspension were diluted up to 100 times in 0.15 M NaCl solution at the same pH, dilution in an identical or more concentrated electrolyte solution protecting the charged aggregates from fragmentation due to the effects of osmotic and electric forces. For polyelectrolyte induced aggregation, the electrolyte free samples were also transferred in a 0.15 M NaCl medium at the same pH. It was assumed that in these two cases further aggregation was impeded by the effect of dilution and that cluster fragmentation during dilution was prevented by the effects of increased ionic strength. The diluted suspension was homogenized under very mild conditions for several minutes. In fact, no influence of shear rate on systematic analysis was detected while maintaining relatively low agitation. On the other hand, it is recognized that aggregates may be disrupted at the inlet of the cell aperture, but due to the coincidence effect, the exact size (mass) of the aggregate is nevertheless recorded.

Our analysis procedure of the histogram furnishes the diameter D_n of the sphere equivalent to the aggregate, as if all the n elementary colloids of diameter D_1 were collapsed in one spherical compact volume. The size n of the colloid is then obtained using the following relationship:

$$n = (D_n / D_1)^3 \tag{1}$$

To determine the characteristics of individual aggregates, the experimental value of the average colloid concentration for each channel i was compared to concentration $V(i)$ calculated using the following relation:[35]

$$V(i) = \frac{\sum_{D_n \in i} \exp\left[-h^2(D_h - D_n)^2/D_n\right]}{\sum_{D_n} \exp\left[-h^2(D_h - D_n)^2/D_n\right]} \tag{2}$$

where h and D_h are fitting parameters: h determines the width of the size distribution, while D_h is the volume average harmonic diameter of the clusters. Concentration $c_n(t)$ of the aggregates constituted of n elementary particles at time t was obtained by assuming the existence of a continuous size distribution and by subdividing the differential curve $V(i)$ in $v(i)$ intervals, the width of each representing the addition of one latex particle to the previous cluster. This procedure made it possible to transform the crude histogram furnished by the particle counter in the corresponding size distribution curve $c_n(t)$ *vs.* n.

Kinetic Aspects in the Aggregation Process. Scaling Approach

In irreversible DLA, the reduced size distribution is calculated on the basis of the following scaling law

$$c_n(t)\, t^{2z} = f(n/t^z) \tag{3}$$

z being obtained from the temporal variation of the second moment or the inverse of the zeroth moment of the cluster size distribution given by

$$N_i = \sum_n n^i c_n(t) \tag{4}$$

In irreversible RLA, a different scaling law

$$c_n(t)\, t^w\, n^\tau = g\,(n/t^z) \tag{5}$$

is found and the different exponents satisfy the scaling relation

$$w = (2-\tau)\, z \tag{6}$$

For the case $\tau > 1$, $N_2(t)$ scales like t^z and $N_0(t)$ scales like t^{-w}. In all situations, we were interested in the variation of $N_2(t)$, and $N_0(t)$. Validity of the scaling approach for aggregation induced by electrolytes and polyelectrolytes thus requires relations (3), (5) and (6) to be verified.

RESULTS AND DISCUSSIONS

Diffusion Limited Aggregation Modes

Relation (3) implies that the characteristics of the systems may be averaged by the behavior of an aggregate of typical size $n \approx t^z$ as assumed in the hierarchical model.[36] According to relation[10]

$$z = [1+(1/D_H)-(d-d_w)/D_H]^{-1} \tag{7}$$

in 3 d (d being the space dimension) and the trajectory dimensionality d_w to be 2 in Brownian coagulation, (D_H being the fractal dimension), one obtains $z = 1$.

The two moments of the cluster size distribution scaling like t are represented in Figure 2 for electrolyte and polyelectrolyte induced aggregation. The different experimental situations are the following:

(i) latex (a) / pH 3.5 / 0.15 M NaCl, (ii) latex (b) pH 3.0 / $9\cdot10^{-4}$ g PVP / g latex

In 0.15 M NaCl medium the colloids aggregate in the primary minimum as evidenced by the energy-distance profile in Figure 3. In the presence of polyelectrolyte, at pH 3.0, $9\cdot10^{-4}$ g PVP / g latex corresponds to the domain where the complex colloid/polymer bears a net surface charge close to zero. For these two experiments, the average sizes scale like t as indicated in Figure 2 and, therefore, $N_2(t)$ or $N_0(t)$ may be used in relation (3) instead of t^z. The variation of the function f is reported in Figure 4. This plot of the asymptotic time behavior of f shows that the given scaling form (3) of the size distribution is consistent with the experimental results. Clearly, aggregations induced by an optimum polymer proportion or by an excess of electrolyte have the same origin. The destabilization of gold colloids by pyridine under fast aggregation conditions has been found to develop in a similar way.[20-23] As $N_2(t)$ and $[N_0(t)]^{-1}$ scale like t, the cluster size polydispersity factor remains constant, $N_2(t)\, N_0(t) / N_1^2$ being of the order of 2 corresponds to the value obtained in cubic lattice simulation (in order to normalize the moment of the size distribution, $N_1(t) = N_1$ was chosen equal to $2.619\cdot10^{12}$, corresponding to one ml latex).

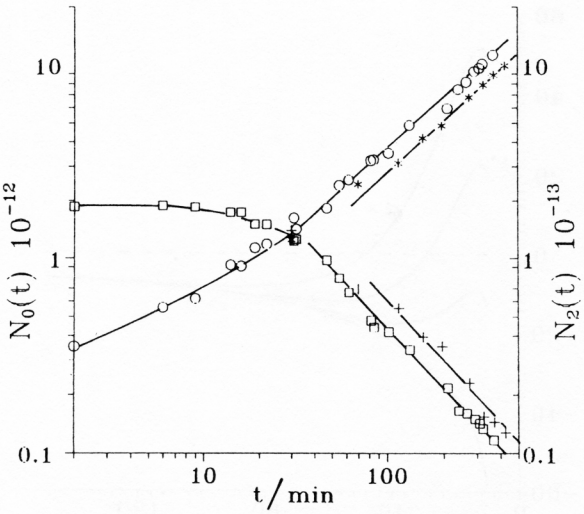

Figure 2. Left ordinate: Number of clusters $N_0(t) = \sum_n c_n(t)$ as a function of aggregation time t (min) (log-log scale): (□) latex (a) /pH 3.5 / 0.15 M NaCl;(+) latex (b) /pH 3.0 / $9 \cdot 10^{-4}$ g pol./g latex. Right ordinate: Second moment of the cluster size distribution $N_2(t) = \sum_n {}^2c_n(t)$ as a function of aggregation time t (min) (log-log scale): (o) latex (a) / pH 3.5 / 0.15 M NaCl; (*) latex (b) / pH 3.0 / $9 \cdot 10^{-4}$ g pol./g latex.

Reaction Limited Aggregation Modes

In the Presence of Electrolytes

By decreasing the ionic strength of the liquid phase from 0.15 to 0.08, 0.05 and 0.03 successively, relation (5) was expected to apply in describing the temporal evolution of the cluster size distribution $c_n(t)$ for latex (a) at pH 3.5. In the asymptotic regime, linear variations of log $N_2(t)$ and log $N_0(t)$ were recorded as a function of log t and the corresponding dynamic scaling exponents z, w and τ (τ being calculated using relation (6)) are reported in Table I (including the exponent determined for 0.15 M NaCl conditions).

Using these exponents, the function g expressed in (5) is reported in Figures 5 and 6 for experiments carried out at 0.03 (τ = 1.65) and 0.05 M NaCl (τ = 1.40, slightly different from 1.56). The reduced size distribution function merges in one unique curve

TABLE I

Electrolyte Induced Aggregation: Latex (a) /pH 3.5/NaCl

Molality	z	w	z–w	τ
0.03	0.655	0.226	0.429	1.65
0.05	0.745	0.326	0.419	1.56–1.40
0.08	0.909	0.655	0.254	1.28
0.15	0.986	0.970	0.016	

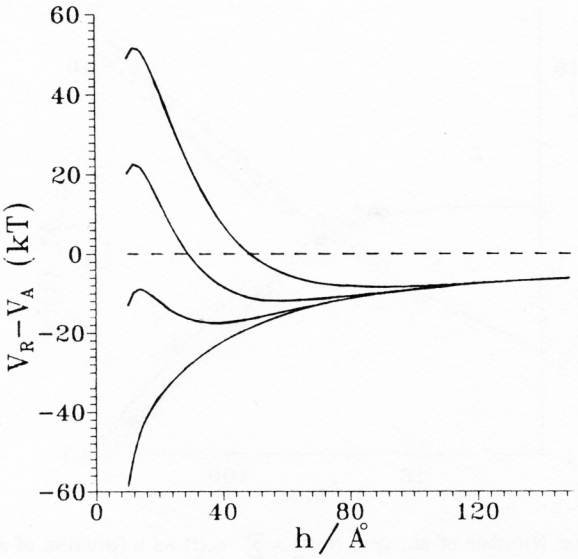

Figure 3. Energy-distance profile for colloids interacting in electrolyte suspension of different concentration, from top to bottom: 0.03, 0.05, 0.08 and 0.15 M NaCl.

all experimental results relating to the entire range of aggregate sizes and the temporal evolution in the asymptotic regime. At each time, the concentration of aggregates of relatively small size (which are present at a maximum concentration), such as $nN_1/N_2(t) < 1$, is described by the following scaling law[17]

$$c_n(t) \approx n^{-\tau} \tag{8}$$

τ being equal or close to $2 - (w/z)$.

Different τ values have been also found in computer simulation studies in the case of RLA involving different collision efficiency P_{ij} between clusters of sizes i and j. The implication is that the collision of colloids does not systematically lead to particle sticking. Assuming σ to be a function of τ, P_{ij} is expressed by

$$P_{ij} = P_o(ij)^{\sigma(\tau)} \tag{9}$$

Reference [16] indicates that τ values smaller than 1.3 correspond to negative values of σ and values larger than 1.3 correspond to positive values of σ. Therefore, the experimental condition of 0.08 M NaCl aqueous suspension sets in a transient aggregation regime for which σ is close to zero. Our interpretation is based on the fact that the rate of disappearance of colloids i and j while forming an aggregate of size $(i+j)$ depends on their mobility, cross sectional area and collision efficiency, P_{ij} (8,16). As in reference [16] the cluster mobility was taken to be size independent, we conclude that in the transient regime the weakened reactivity of small clusters opposes the influence on the aggregation rate of the large mobility of small clusters while the inverse phenomenon is valid for large aggregates. As a result, mobility and reactivity may appear to be strictly size independent.

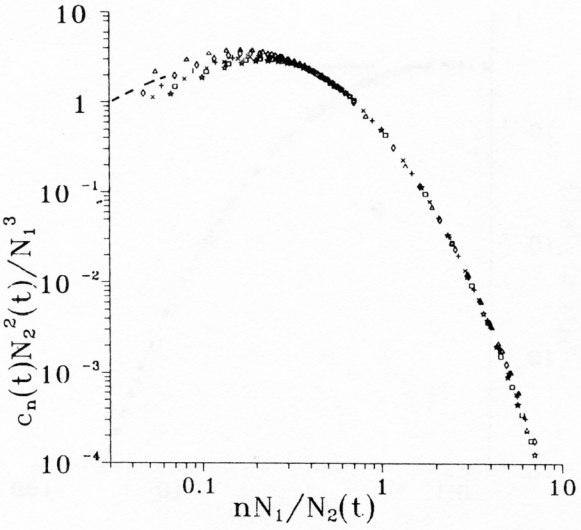

Figure 4. Reduced size distribution curve (relation (3) corresponding to fast aggregation conditions in the asymptotic regime for NaCl induced aggregation: latex (a) / pH 3.5 / 0.15 M NaCl and PVP induced aggregation: latex (b) / pH 3.0 / $9 \cdot 10^{-4}$ g pol./g latex.

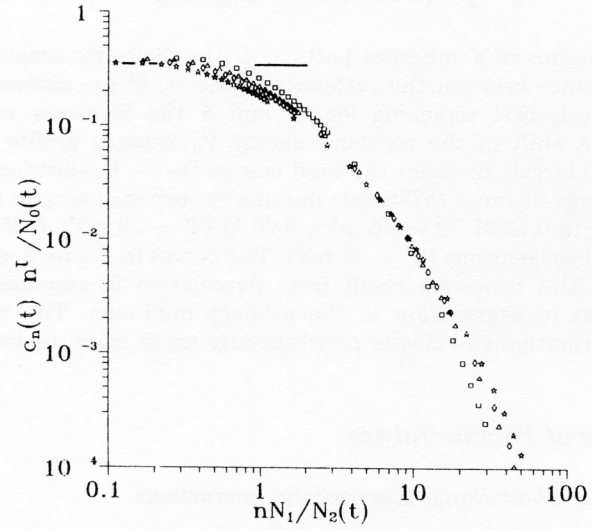

Figure 5. Reduced size distribution curve (relation (5) corresponding to poor aggregation conditions in the asymptotic regime for NaCl induced aggregation: latex (a) / pH 3.5 / 0.03 M NaCl.

In the presence of electrolytes, the variable cluster reactivity $\sigma(\tau)$ is governed by the ionic strength of the suspending medium, which controls the Debye-Hückel screening length. Therefore, van der Waals attractive forces are differently opposed by Coulombic repulsive forces as expressed by

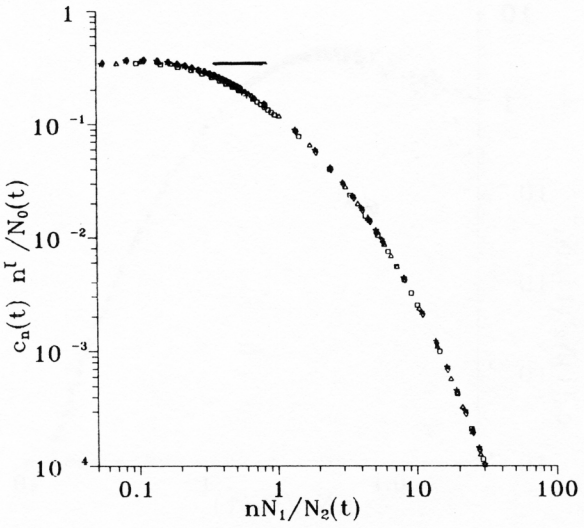

Figure 6. Reduced size distribution curve (relation (5) corresponding to poor aggregation conditions in the asymptotic regime for NaCl induced aggregation: latex (a) / pH 3.5 / 0.05 M NaCl.

$$V_R - V_A = (Da\Psi^2/2)\ln[1+\exp(-\kappa h)] - Aa/12h \qquad (10)$$

where a is the radius of a spherical particle, D the dielectric constant of the double layer, h the distance between the surfaces of spheres, Ψ the surface potential, κ the Debye-Hückel reciprocal screening length and A the Hamaker constant equal to $0.65 \cdot 10^{-13}$ erg. A shift of the repulsive energy V_R-distance profile (imposed by the terms Ψ and κh) largely modifies the total energy ($V_R v - V_A$)-distance curve. Figure 3 portrays the energy-distance (kT-angstrom) profile corresponding to colloid/colloid interaction energy in 0.15 M (Ψ =–15 mV), 0.08 M (Ψ =–20 mV). 0.05 M (Ψ =–22 mV) and 0.03 M NaCl suspensions (Ψ =–23 mV). The curves in Figure 3 evidence that electrolyte induced RLA processes result from flocculation in secondary minima while DLA corresponds to aggregation in the primary minimum. The very different aggregate size distribution and cluster polydispersity result from the two mechanisms of aggregation.

In the Presence of Polyelectrolytes

Mode of Action of Short Range Electrostatic Interactions

At pH 3.0, the carboxylic acid groups of the latex (b) surface are ionized and the degree of protonation of the polymer pyridine groups is equal to 0.475. The amount of PVP adsorbed at full surface coverage was found to be $20.75 \cdot 10^{-4}$ g pol./g latex. Fast DLA of the polymer/colloid complex occurred when adsorption of 7 to $9 \cdot 10^{-4}$ g PVP / g latex (about one third of the total adsorption) conferred a net surface equal to zero. A sketch of the interfacial layer would represent the polyelectrolyte backbone close to the colloid surface, the contact points being the ion-pairs [–$COO^- \cdots {}^+HN$–] formed by the carboxyl groups of the colloid and the pyridinium group of the polymer.

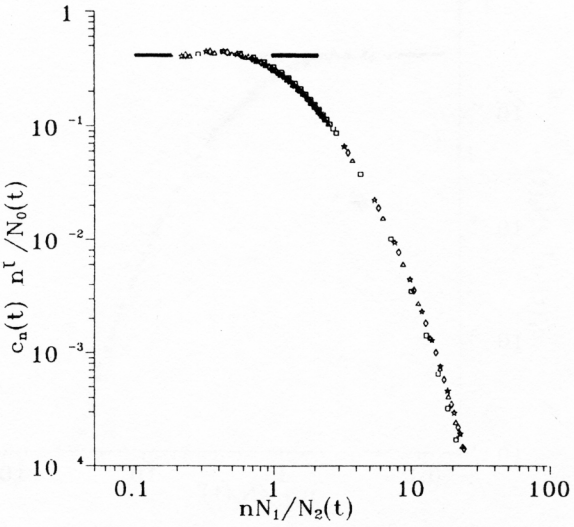

Figure 7. Reduced size distribution curve (relation (5)) corresponding to poor aggregation conditions in the asymptotic regime for PVP induced aggregation: latex (b) / pH 3.0 / 0.7 (τ = 1.55) and $3.5 \cdot 10^{-4}$ g pol./g latex (τ = 1.44). Aggregation in the presence of a default of adsorbed polymer.

We now consider the situation of incomplete charge screening of the colloid/polymer complex. Slow aggregation was observed when (i) the colloid surface charges were partially screened (default of adsorbed polymer) and (ii) the colloid/polymer complex developed the residual charge on a »excess« of adsorbed polyelectrolyte. Experiments were performed at pH 3.0 for the polymer dosages 0.7, 3.5 and $4.9 \cdot 10^{-4}$ g/g (default of adsorbed polymer) and 12 and $14 \cdot 10^{-4}$ g/g (»excess« of polymer).

Linear variations of $\log N_2(t)$ and $N_0(t)$ were found for the different systems in the asymptotic regime and the scaling exponents z and w, the polydispersity factor $(z - w)$, exponent τ are reported in Table II (results of the DLA process corresponding to a surface coverage of $9 \cdot 10^{-4}$ g PVP/g latex are included).

TABLE II

Polyelectrolyte induced aggregation: charge-charge interaction. latex (b) pH 3.0/PVP

Polym Conc. g/10^{-4} g latex	z	w	z–w	τ
0.7	0.642	0.286	0.356	1.55
3.5	1.016	0.573	0.443	1.44
4.9	1.076	0.808	0.268	1.25
9.0	1.000	1.000	0.000	–
12.0	1.000	0.900	0.100	1.10
14.0	1.059	0.352	0.707	1.67
20.7	full surface coverage – stable colloid/polymer complex			

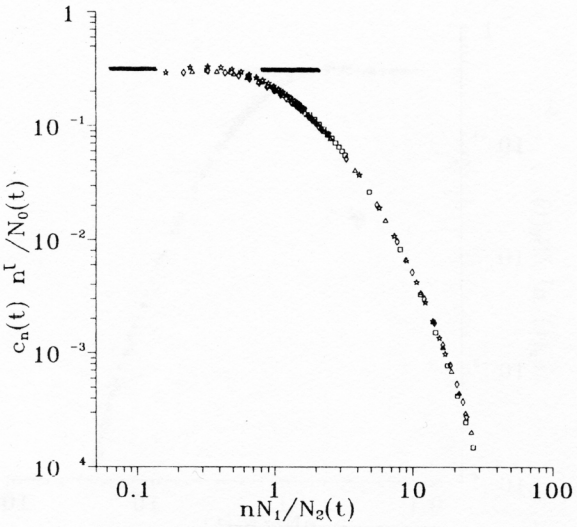

Figure 8. Reduced size distribution curve (relation (5) corresponding to poor aggregation conditions in the asymptotic regime for PVP induced aggregation: latex (b) / pH 3.0 / $14 \cdot 10^{-4}$ g pol./g latex (τ = 1.55). Aggregation in the presence of an »excess« of adsorbed polymer.

The temporal variation of the corresponding reduced size distributions, represented in Figure 7 ($0.7 \cdot 10^{-4}$ and $3.5 \cdot 10^{-4}$ g/g) and Figure 8 ($14 \cdot 10^{-4}$ g/g) by a unique curve, ratifies the validity of the dynamic scaling approach. We note a variable aggregate reactivity depending on the colloid surface coverage and, on the other hand, a critical τ value of 1.25 is recorded for a surface coverage of $4.9 \cdot 10^{-4}$.

It is, however, important to note that if polyelectrolytes are used to neutralize the colloid surface charge, strong effects result from slight modifications of the surface characteristics. Actually, the bare latex is stable in aqueous suspension at pH 3.0 and a surface coverage of 7 to $9 \cdot 10^{-4}$ g/g is sufficient to form a neutral polymer/colloid complex. Typically, at $4.9 \cdot 10^{-4}$ the complex resembles the »electrostatic patch« model of Gregory,[37] where, on the average, one half is positively charged and the other half is negatively charged. In the spirit of the model of La Mer, only one half of the interparticle collisions can be efficient towards sticking. A mean value of 1.25 is found for τ and we believe that the interaction between positively and negatively charged surface groups belonging to two colliding particles is responsible for the size independent cluster reactivity. For the smaller surface coverage of 3.5 and $0.7 \cdot 10^{-4}$ g/g, the cluster reactivity should be differently size dependent, as indicated in Table II.

The scheme is slightly different in the case of an »excess« of polymer. At a coverage of $14 \cdot 10^{-4}$ g/g the net positive charge of the colloid/polymer corresponds to about one half of the negative charge initially present on the bare colloid. This charge is smeared over the colloid surface and creates a positive surface potential Ψ. Therefore, as the experiments were carried out at a constant ionic strength, it is obvious that in relation (10) the surface potential term only varies with the »excess« of polymer adsorbed. Hence, it is expected that the aggregation develops with features of variable cluster reactivity and the presentation of τ as a function of the polymer dosage in Figure 9 substantiates our argumentation.

TABLE III

Polyelectrolyte Induced Aggregation: Bridging Mechanism

Polym Conc. g/·10^{-4} g latex	z	w	z–w	τ
0.7	0.551	0.269	0.282	1.51
2.1	0.854	0.460	0.394	1.46
4.9	0.924	0.443	0.481	1.52
7.0	0.981	0.557	0.424	1.43–1.50
9.0	1.007	0.460	0.547	1.54
12.0	0.720	0.286	0.434	1.60
14.0	0.443	0.139	0.304	1.69

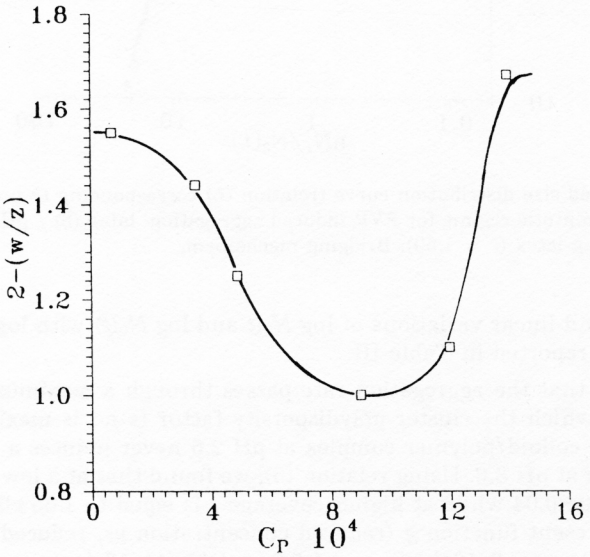

Figure 9. Presentation of $t = 2-(w/z)$ as a function of the polyelectrolyte concentration for aggregation of latex (b) at pH 3.0. Charge-charge interactions.

Mode of Action of the Interparticle Bridging Mechanism

In the preceding situation, the interfacial polyelectrolyte layer adopted a relatively flat conformation and consideration of the effects of short range electrostatic forces permitted us to interpret the mechanism of the aggregation processes, which showed some similarity with the reaction limited electrolyte induced aggregation. To investigate the second mode of action of adsorbed polyelectrolytes and to trigger polymer bridging, experiments were performed at pH 2.5 where the ionic surface of the latex is close to zero and the polymer highly ionized. As a result, the structure of the polyelectrolyte resembles a set of loops protruding extensively in the liquid phase and having only a·small number of pyridinium groups in the surface plane (this model is valid as long as no interfacial reconformation modifies the initial conformation.[32] Like previously, the aggregation was studied as a function of the amount of polymer adsor-

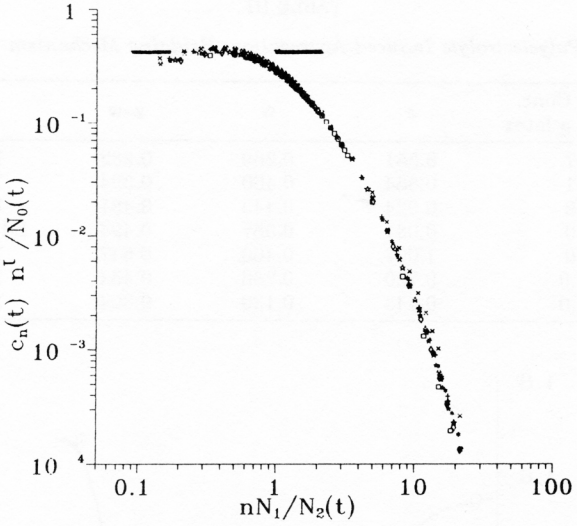

Figure 10. Reduced size distribution curve (relation (5) corresponding to poor aggregation conditions in the asymptotic regime for PVP induced aggregation: latex (b) / pH 2.5 / 4.9 (t = 1.50) and $7 \cdot 10^{-4}$ g pol./g latex (τ = 1.50). Bridging mechanism.

bed at pH 2.5 and linear variations of log $N_2(t$ and log $N_0(t)$ with log t were obtained. The results are reported in Table III.

It is shown that the aggregation rate passes through a maximum at a given concentration, for which the cluster polydispersity factor (z–w) is maximal. It is worthy of note that the colloid/polymer complex at pH 2.5 never induces a DLA process, unlike the complex at pH 3.0. Using relation (6), we found that at a low surface coverage, τ is equal to 1.50±0.04 while at higher coverage τ is equal to 1.65±0.05. These values are used to represent function g (reduced concentration *vs*, reduced size) as reported in Figure 10 (4.9 and $7.0 \cdot 10^{-4}$ g/g; τ = 1.50) and 11 ($14 \cdot 10^{-4}$ g/g; τ = 1.65) according to relation (5). In Figure 12, master curves g are reported for the different polymer dosages of 0.7, 1.2, 4.9, 7.0, 9.0 and $12.0 \cdot 10^{-4}$ g pol. / g latex. A unique function g describes in terms of reduced variables the temporal evolution of the cluster size distribution.

Establishment of interparticle bridges involves interaction between the pyridinium group of the polymer chain and the carboxylic acid group localized in the colloid surface. Ion-pairing between the two groups is only established by virtue of charge-charge attraction exerted at a short distance while the corresponding colloids may be separated by distances for which van der Waals attractive forces play no role. We have only to examine the surface accessibility to a polymer coil adsorbed on the surface of another colloid. A lower reactivity is determined below a threshold coverage of about $8.0 \cdot 10^{-4}$ g/g. To interpret the existence of different reactivity of the colloid/polymer complex, we look at the mechanism of PVP adsorption on the colloid surface and assume that the processes involved in colloid filling by isolated polymer coils may exist for a coil already attached to one particle and adsorbing on another colloid. We previously investigated the characteristics of the PVP adsorption as a function of the rate of polymer supply to the colloid surface.[32] In fact, for instantaneous mixing of colloid

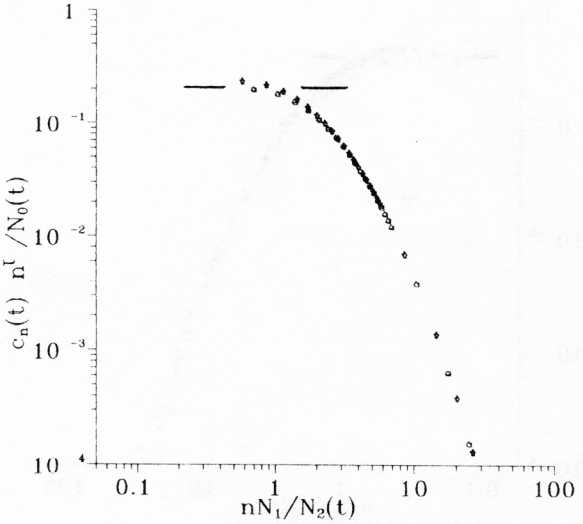

Figure 11. Reduced size distribution curve (*cf* relation (5) corresponding to poor aggregation conditions in the asymptotic regime for PVP induced aggregation: latex (b) / pH 2.5 / $14 \cdot 10^{-4}$ g pol./g latex (t = 1.60). Bridging mechanism.

and polymer, the kinetic coefficient of the adsorption process corresponds to that calculated by a simulation technique using the random sequential adsorption plus the in-plane diffusion model.[38] We calculated that only about one third of the available surface could be covered by solute macromolecule at a relatively fast rate while the remaining surface needs a long time to be fully covered. This implies that the accessibility of the carboxylic acid surface groups may be very different below and above this threshold coverage close to $8 \cdot 10^{-4}$ g/g. This interpretation completes the other previously given, which was based only on the different reactivity of acid-base groups under small and large surface coverages.[39]

CONCLUSION

Direct tests of the dynamic scaling for $c_n(t)$ were carried out by counting the colloids at several intervals during the aggregation process. Two kinds of plots for the reduced size distribution have been obtained: for DLA, $c_n(t)$ exhibits a well-defined peak as a function of n while it decreases continuously as n for RLA. For electrolyte and polyelectrolyte induced aggregation the cluster size frequency is represented by a single curve in both cases.

However, the mechanisms of the colloid destabilization and the cluster reactivity are very different when charge-charge interactions are effective, as compared to polymer bridging. Charge screening effects develop at relatively large distances. Collision efficiency may be continuously varied by changing the electrolyte concentration in the suspending medium or the amount of the polyelectrolyte adsorbed on the colloid. In fact, modification of the Debye-Hückel screening length or the net charge of the colloid/polymer complex modulates the energy-distance profile for interacting colloids. In contrast, the intrinsic rate of the establishment of polymer bridges between active sites

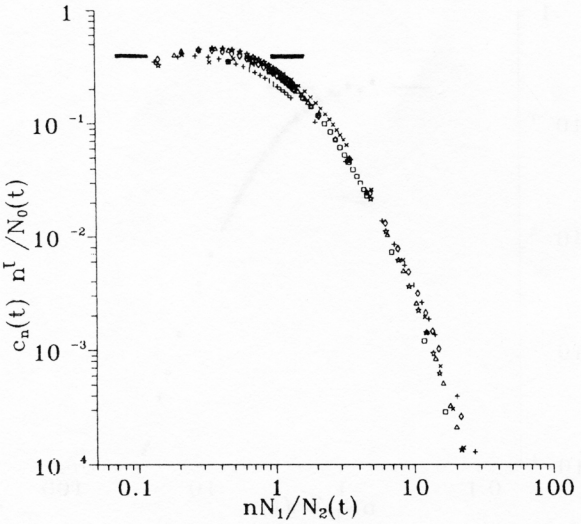

Figure 12. Reduced size distribution curve (master curve) corresponding to poor aggregation conditions in the asymptotic regime for PVP induced aggregation: latex (b) / pH 2.5 / and different PVP concentration: 0.7, 2.1, 4.9, 7.0, 9.0 and $12 \cdot 10^{-4}$ g pol./g latex. Bridging mechanism.

located on the colloid surface and functional groups of the polymer chains is relatively constant; it is slightly modified when a comparison is made for low and high degrees of surface coverage.

In all situations, the influence of electrolyte and polymer dosage on colloid aggregation dynamics is well described in terms of the scaling exponents w and z. Moreover, cluster reactivity (as expressed by the scaling parameter τ) and concentration of the destabilizing agent exert a complementary and complex influence on the temporal evolution of the cluster size distribution and the aggregate size polydispersity. General agreement is found with the dynamic scaling laws determined by computer simulation and our experimental results demonstrate the validity and the richness of this approach to apprehend the dynamics of colloid destabilization in multiple situations where electrolyte and polyelectrolyte are found to induce well differentiated aggregation mechanisms.

Acknowledgments. – The author is grateful to Dr C. Pichot and Dr G. Graillat of the Laboratoire des Materiaux Organiques (Lyon-France) for kindly providing the lattices. The author thanks Dr R. Varoqui, Dr A. Elaissari and Dr S. Stoll, who have helped him to develop a better understanding of experimental results. Experimental and technical assistance of J. Widmaier and G. Maennel is acknowledged. This work was performed with the financial support of the PIRSEM/PIRMAT ARC »Flocculation« (CNRS).

REFERENCES

1. M. von Smoluchowski, *Phys. Z.* **17** (1916) 593.
2. T. A. Witten and S. M. Sander, *Phys. Rev. Lett.* **47** (1981) 1400.
3. P. Meakin, *Phys. Rev. Lett.* **51** (1983) 1119.
4. M. Kolb, R. Botet, and R. Jullien, *Phys. Rev. Lett.* **51** (1983) 1123.

5. P. Meakin and J. M. Deutch, *J. Chem. Phys.* **80** (1984) 2115.
6. T. Vicsek and F. Family, *Phys. Rev. Lett.* **52** (1984) 1669.
7. H. G. E. Hentschel and J. M. Deutch, *J. Chem. Phys.* **81** (1984) 2496.
8. P. Meakin, T. Vicsek, and F. Family, *Phys. Rev.***31** (1984) 564.
9. M. Kolb, *Phys. Rev. Lett.* **53** (1984) 1653.
10. R. Botet and R. Jullien, *J. Phys.* **A17** (1984) 2517.
11. R. M. Ziff, E. D. McGrady, and P. Meakin, *J. Chem. Phys.* **82** (1985) 5269.
12. P. Meakin, *J. Colloid Interface Sci.* **102** (1984) 491; **102** (1984) 505.
13. R. Jullien, M. Kolb, and R. Botet, in *Kinetics of Aggregation and Gelation* edited by F. Family and D. P. Landau, North-Holland, Amsterdam, 1984.
14. M. Kolb, and R. Jullien, *J. Phys. Lett.* **45** (1984) L977.
15. R. Jullien and M. Kolb, *J. Phys.* **A17** (1984) L639.
16. F. Family, P. Meakin, and T. J. Vicsek, *J. Chem. Phys.* **83** (1985) 4144.
17. W. D. Brown and R. C. Ball, *J. Phys.* **A18** (1985) L517.
18. P. Meakin, and F,. Family, *Phys. Rev.* **A36** (1987) 5498.
19. C. Allain and B. Jouhier, *J. ys.* **44** (1983) 421.
20. D. A. Weitz and M. Oliveria, *Phys. Rev. Lett.* **52** (1984) 1433.
21. D. A. Weitz, J. S. Huang, M. Y. Lin, and J. Sung, *Phys. Rev. Lett.* **53** (1984) 1657.
22. D. A. Weitz, J. S. Huang, M. Y,. Lin, and J. Sung, *Phys. Rev. Lett.* **54** (1985) 1416.
23. D. A. Weitz and M. Y. Lin, *Phys. Rev. lett.57 (1986) 2037.*
24. C. Camotti, P. Codastefano, and P. Tartaglia, *Europhys. Lett.* **5** (1988) 703.
25. J. F. Roussel, R. Blanc, and C. Camoin *Compt. Rend. Acad. Sci. Ser. 2* **306** (1988) 467.
26. E. Pefferkorn, C. Pichot, and Varoqui, *J. Phys. (Les Ullis)* **49** (1988) 983.
27. J. C. Earnshaw and D. J. Robinson, *Progr. Colloid Polym. Sci.* **79** (1989) 162.
28. J. Gregory, *J. Trans. Faraday Soc.* **65** (1969) 2260.
29. R. Varoqui and E. Pefferkorn, *Progr. Colloid Polym. Sci.* **79** (1989) 194.
30. J. Gregory, in *The Scientific Basis of Flocculation* edited by K. J. Ives, Sijthoff & Noordhoff, Alphen aan den Rijn, The Netherlands 1978, p 101.
31. B. Vincent, *Adv. Colloid Interface Sci.* **4** (1982) 193.
32. A. Elaissari and E. Pefferkorn, *J. Colloid Interface Sci.* **138** (1990) 187.
33. J. W. Goodwin, R. H. Ottewill, R. Pelton, G. Vianetta, and D. E. Yates, *Br. Polym. J.* **10** (1978) 173.
34. P. H. Walker and J. Hutka, *Division of Soils*, Technical Paper No. 1,3 (1971).
35. J. M. Keynes (Lord Keynes), *Principal Averages and the Laws of Error which lead to them*, J. R. S. S. **74** (1910–1911) 324.
36. R. Botet, R. Jullien, and M. Kolb, *J. Phys.* **A17** (1984) L75.
37. J. J. Gregory, *Colloid Interface Sci.* **42** (1973) 448.
38. A. Elaissari, A. Haouam, C. Huguenard, and E. Pefferkorn, *J. Colloid Interface Sci.* ***149*** (1992) 68.
39. A. Elaissari, and E. Pefferkorn, *J. Colloid Interface Sci.* **143** (1991) 343.

SAŽETAK

Agregacija koloida inducirana elektrolitom i polielektrolitom. Mehanizam koloidne destabilizacije

E. Pefferkorn

Sferne čestice lateksa poslužile su kao model koloida za ispitivanje procesa agregacije, koja je posljedica djelovanja elektrolita i polielektrolita. Raspodjela veličina koloida mjerena je direktno tehnikom brojila čestica za difuzijom limitiranu agregaciju (DLA). Očekivane su zvonolike krivulje (krivulje s maksimumom), gdje sljepljivanje čestica slijedi nakon svakoga međučestičnog sudara. Frekvencija veličina koloida trebala bi biti opisana krivuljom koja kontinuirano pada, ako

se očekuje reakcijom limitirana agregacija (RLA). Posljednji proces uključuje da djelotvornost sudara može ovisiti o veličini agregata kojim je slijedilo sljepljivanje čestica.

Izračunani su različiti momenti raspodjele veličina, počevši od distribucije nakupina.

Kad se međučestične interakcije moduliraju elektrostatskim silama u prisutnosti suviška elektrolita ili pri takovoj koncentraciji polimera koja inducira brzu agregaciju, reducirana raspodjela veličina pokazuje tipični maksimum, a agregacijska kinetika opisana je jednostavnim skalnim zakonom. Rezultat je taj da vremenski nepromjenljiva veličina polidisperznost karakterizira logaritamsko vremensko ponašanje. Neovisno o tim idealnim koagulacijskim uvjetima, flokulacija se odvijala manjom brzinom, a dinamički skalni zakoni zahtijevali su dva skalna eksponenta, w i z. Faktor polidisperznosti veličine nakupina rastao je s agregacijskim periodom što je bila posljedica varijabilne djelotvornosti sudara.

Kada je fleksibilni polimer djelovao kao međučestični premošćujući agens, količina polimera adsorbirasnog na koloidnoj površini također je djelovala na brzinu agregacije, ali sam način agregacije bio je određen samo interakcijom između polimera i koloida.

Za brzu agregaciju nađeno je da inducira maksimalnu polidisperznost veličine nakupina. U svima tim situacijama načini koloidne agregacije analizirani su upotrebljavajući rezultate kompjuterske simulacije agregacije nakupina-nakupina, a eksperimentalni rezultati prikazani su skalnim prikazom.

Valjanost skalnih relacija bila je verificirana za agregaciju induciranu elektrolitom i polielektrolitom, a različiti procesi odgovarali su difuzijski i reakcijski limitiranoj agregaciji.